

---

## Zinc isotopes as tracers of anthropogenic sources and biogeochemical processes in contaminated mangroves

Ferreira Araujo Daniel <sup>1,2,3,\*</sup>, Machado Wilson <sup>4</sup>, Weiss Dominik <sup>5</sup>, Mulholland Daniel S. <sup>6</sup>,  
Garnier Jeremie <sup>3</sup>, Souto-Oliveira Carlos E. <sup>1</sup>, Babinski Marly <sup>1</sup>

<sup>1</sup> Universidade de São Paulo, Instituto de Geociências, Rua do Lago 562, Cidade Universitária, São Paulo, Brazil

<sup>2</sup> Laboratoire de Biogéochimie des Contaminants Métalliques, IFREMER, Centre Atlantique, F44311, Nantes Cedex 3, France

<sup>3</sup> Laboratoire Mixte International-Observatoire des changements Environnementaux –LMI-OCE, Institut de Recherche pour le Développement (IRD) / Universidade de Brasília, Campus Darcy Ribeiro, Brasília, Brazil

<sup>4</sup> Universidade Federal Fluminense, Departamento de Geoquímica, Campus do Valonguinho, Niterói, Rio de Janeiro, Brazil

<sup>5</sup> Imperial College London, Earth Science and Engineering, London, United Kingdom

<sup>6</sup> Universidade Federal do Tocantins, Departamento de Química Ambiental, Rua Badejós, Lote 7, Chácaras 69/72, Zona Rural, Gurupi, Tocantins, Brazil

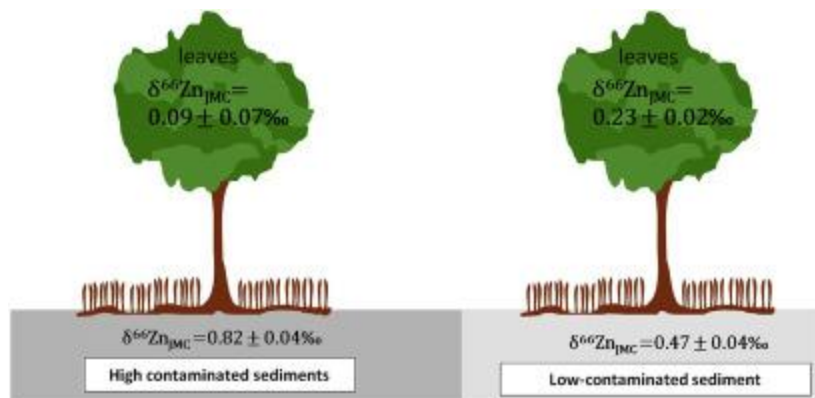
\* Corresponding author : Daniel Ferreira Araujo, email address : [danielunb.ferreira@gmail.com](mailto:danielunb.ferreira@gmail.com)

---

### Abstract :

Recent work has shown that variations in zinc (Zn) isotope ratios enable us to identify contamination sources in the terrestrial environment and uptake processes in higher plants. Here in this study, we demonstrate that this also holds true for mangrove forests, which play an important role in the biogeochemical cycling of metals in tropical coastal ecosystems and that are seriously threatened by anthropogenic pollution. To this end, we determined zinc concentration and isotope composition (expressed using the  $\delta^{66}\text{Zn}$  notation relative to the JMC 3-0749-L standard) in sediments and tree leaves collected from a mangrove close to Rio de Janeiro in Brazil. The  $\delta^{66}\text{Zn}_{\text{JMC}}$  values of sediments vary between +0.36 and +0.84‰ and fall on a mixing line between detrital terrestrial sources (characterized with  $\delta^{66}\text{Zn}_{\text{JMC}} = +0.28 \pm 0.12\text{‰}$ ,  $2\sigma$ ) and metallurgical ore sources ( $\delta^{66}\text{Zn}_{\text{JMC}} = +0.86\text{‰} \pm 0.15\text{‰}$ ,  $2\sigma$ ). Leaves of *Laguncularia racemosa*, in contrast, showed  $\delta^{66}\text{Zn}_{\text{JMC}}$  values ranging between +0.08 and +0.23‰, suggesting that processes including uptake, translocation and bioavailability in the rhizosphere control the isotope composition of zinc in the mangrove plant.

## Graphical abstract



## Highlights

► The  $\delta^{66}\text{Zn}_{\text{JMC}}$  values of mangrove sediments suggest a mixing source processes. ► Leaves of *Laguncularia racemose* showed  $\delta^{66}\text{Zn}_{\text{JMC}}$  values ranging between +0.08 and +0.23‰. ► Zn uptake, translocation and bioavailability control the isotope composition of leaves. ► Zn isotope compositions of leaves may indicate environmental changes in mangrove systems.

**Keywords** : Metal transition isotopes, Metal contamination, Mass spectrometry, Coastal ecosystems, Mangrove leaves

## 43 **1. Introduction**

44 Mangrove forests are found in the inter-tidal region between sea and land in tropical and  
45 subtropical regions of the world, growing typically under harsh environmental conditions  
46 such as high salinities, elevated temperatures, extreme tides, high sedimentation rates and  
47 muddy anaerobic soils (Alongi et al., 2008; Giri et al., 2010; Bayen et al., 2012). These

48 unique forests are among the most productive ecosystems in the world and provide valuable  
49 food, energy sources and raw materials for the local economies (Giri et al., 2010; Agardy  
50 and Alder, 2010; Marchand et al., 2016).

51 Mangroves shelter many species of economic and ecological value such as  
52 mammals, birds, reptiles and insects (Nagelkerken, 2008). Epibionts (tunicates, sponges,  
53 algae, and bivalves) and in- and epi-faunal species (prawns and crabs) live in the roots-  
54 sediment mangrove system (Nagelkerken, 2008). The complex mangrove food web is  
55 supported by recycling of tree leaves, which once converted into detritus by decomposers  
56 serve as food to primary consumers as plankton, epiphytic algae and microphytobenthos  
57 (Nagelkerken, 2008; Castro and Huber, 2010).

58 Despite mangroves supporting a wide variety of ecosystem services and being  
59 economically valuable (up to several thousand US\$ yr<sup>-1</sup> ha<sup>-1</sup>, Walters et al., 2008), they  
60 remain one of the world's more threatened tropical environments (Valiela, 2001). It is  
61 estimated that human activities have led to a loss of at least 35% of the world's mangrove  
62 area due the conversion to mariculture, agriculture, urbanization and to other activities  
63 (Valiela, 2001).

64 Environmental pollution has played an important factor in the degradation of  
65 mangroves (Lewis et al., 2011; Bayen et al., 2012; Sandilyan and Kathiresan, 2014). Urban  
66 sprawl combined with industrial expansion has led to the release of toxic metals and  
67 metalloids into the mangrove environments (Machado and Lacerda, 2004; Lewis et al.,  
68 2011; Da Souza et al., 2014; Marchand et al., 2016; Araújo et al., 2017d). Depending on  
69 bioavailability and speciation, these elements are incorporated into bio-geosphere cycles.  
70 Essential elements (e.g., Zn, Cu, Mo) play an important biological role and participate in a  
71 wide range of important cellular biochemical reactions (Reilly, 2004). At high

72 concentrations, however, these elements lead to reduction of photosynthesis in mangrove  
73 plants and of growth and biomass, and finally induce mortality (Adriano and Adriano,  
74 2001; Sparks, 2005; Bayen et al., 2012 and references therein; Alongi, 2017).

75         Since metal contaminations of mangroves may pose major risks to biota and human  
76 health, developing tools to trace anthropogenic sources and to identify plant responses to  
77 environmental stress triggered by metal contamination is of great interest. To this end, the  
78 application of stable isotope ratios is promising for zinc (Zn). Firstly, they fractionate  
79 during industrial processes (e.g., metallurgy and combustion by high-temperature or  
80 electrolysis processes) resulting in fingerprints isotopically distinct for man-made materials  
81 and by-products from those found in nature (Kavner et al.; 2008; Sivry et al., 2008; Borrok  
82 et al.; 2010; Ochoa and Weiss, 2015; Thapalia et al., 2015; Yin et al.; 2015), which allows  
83 to use Zn isotope ratios to discriminate between natural and anthropogenic sources in  
84 marine, terrestrial and atmospheric compartments (Yin et al., 2016; Souto-Oliveira et al.,  
85 2018). Secondly, Zn isotope fractionation occurs during uptake, translocation and  
86 distribution between the internal compartments of plants (Viers et al., 2007; Moynier et al.,  
87 2009; Caldelas et al., 2011; Jouvin et al., 2012; Arnold et al., 2015). These processes seem  
88 dependent on plant uptake strategies, concentration, speciation, redox conditions,  
89 transpiration flow and height (Moynier et al., 2009; Couder et al., 2015; Caldelas and  
90 Weiss, 2017).

91         To date, only a few studies have explored isotope fractionations of Zn during the  
92 biogeochemical cycling in terrestrial or wetland ecosystems (Viers et al., 2007; Aucour et  
93 al., 2015; Viers et al., 2015; Aucour et al., 2017). To this end, we conducted a preliminary  
94 study of Zn isotope variations in mangrove sediment-plant systems in Sepetiba Bay, a site  
95 historically impacted by Zn-enriched wastes from an old electroplating plant (Molisani et

96 al., 2004). Previous studies of our group testing Zn isotopes as tools to discriminate and  
97 quantify the relative contributions of natural and anthropogenic Zn sources to Sepetiba Bay  
98 focused on mud flat sediments, suspended particulate matter and a single mangrove  
99 sediments core located close to the old electroplating plant (Araújo et al., 2017a, c). This  
100 complementary study focuses on sediments and leaves of mangrove trees (*L. racemosa*)  
101 collected from sampling locations with different extent of Zn contamination. The specific  
102 questions addressed during this study are: (i) do mangrove sediments record the isotope  
103 compositions of pollutant sources? (ii) do mangrove trees fractionate Zn isotopes during  
104 uptake and transport to aerial tissues? If so, (iii) which are the possible effects of  
105 concentration, speciation, bioavailability and physiological processes (uptake,  
106 translocation, tolerance mechanism) on the Zn isotopes composition of the mangrove  
107 leaves?

108

## 109 **2. Study area**

110 The study was conducted in Sepetiba Bay (southeastern Brazil), a micro tidal estuary type  
111 lagoon, located 60 km west from Rio de Janeiro city (Fig.1). Nine rivers drain an extensive  
112 watershed of approximately 2,654 km<sup>2</sup>, which includes agricultural, industrial and urban  
113 areas. The main river (Guadu River) reach the bay through artificial channels, which among  
114 them, the São Francisco channel, with an annual flow of  $6.5 \times 10^9$  m<sup>3</sup>, is responsible for  
115 over 86% of the total freshwater input (Molisani et al., 2004). Mangrove forests extend  
116 along the bay shore, providing nursery and feeding areas for the bays fisheries. The  
117 dominant tree species are red mangrove (*Rhizophora mangle*), black mangrove (*Avicennia*  
118 *shaueriana*) and white mangrove (*Laguncularia racemosa*).

119 In the 1960's, an electroplating plant started to operate close the northeastern shore  
120 (Fig.1). The zinc purification process used silicate ores (calamine:  $Zn_2SiO_3(OH)_2$  and  
121 willemite:  $SiO_4Zn_2$ ) acquired from Vazante (Minas Gerais, Brazil), the most important Zn  
122 deposit in Brazil (Barone, 1976). The waste produced during the ore refining processes  
123 were exposed to the open air and lixiviated during rainfalls, reaching surrounding  
124 mangroves and the bay through a small tidal creek located in the Saco do Engenho  
125 mangrove, considered as the *hot spot* area (Fig.1) (Molisani et al., 2004). The amounts of  
126 zinc and cadmium remobilized from the waste were estimated to be about  $24 \text{ t y}^{-1}$  for Cd  
127 and  $3,660 \text{ t y}^{-1}$  for Zn (Molisani et al., 2004). Despite the end of zinc refining operations in  
128 1997 and the removal of the waste in 2012, Zn-enriched sediment particles from the *hot*  
129 *spot* continue to be remobilized throughout the bay during tidal cycles (Araújo et al., 2017a;  
130 Araújo et al., 2017c). Computational modeling of the lagoon hydrodynamics suggests a  
131 trend of fine sediments deposition along the northeastern coastal area of the bay where the  
132 tidal flats and mangroves acts as sinks of contaminants (Montezuma, 2013).

133

### 134 3. Materials and Methods

#### 135 3.1 Sampling and sample preparation

136 Surface sediments were collected at three different mangrove sites (Fig.1), during low tide  
137 in 2008. The first site is located in the Saco do Engenho (station A), the second site is  
138 located close the mouth of São Francisco channel (station B) and the third site is located in  
139 the mangrove of Enseada das Garças (station C). The latter site is located within an  
140 environmental protection area surrounded by urbanized and landfill areas. At each sampling  
141 site, three superficial ( $\sim 0\text{-}5 \text{ cm}$  depth) surface sediment replicates were sampled and

142 packed into polyethylene bags. The samples were dried at 40 °C, crushed and sieved at 63  
143 µm. This grain size fraction (<63 µm) was used for elemental and isotopic analyses.

144 At the three sampling sites, *L. racemosa* trees colonize the sediments. *Laguncularia*  
145 *racemosa* leaves were sampled in triplicate from trees surrounding the sampled sediments.  
146 The leaves were stored in plastic bags until the return to the laboratory and then washed  
147 using ultrapure water. These samples were dried at 80°C during 24 h and finely ground for  
148 homogenization. Surface sediment samples and certified materials (BCR-2 and BHVO-2  
149 basalts from the US Geological Survey and 1646a estuarine sediment from National  
150 Institute for Standards and Technology, NIST) were weighed in Savillex® Teflon beakers  
151 and digested on a hot plate using a multiple-step acid procedure with HF, HNO<sub>3</sub>, HCl. Leaf  
152 samples and a plant certified reference material (1573a tomato leaves from NIST) were  
153 digested using a microwave system (Speedwave 4, Berghof) and concentrated acid mixing  
154 (HF, HCl and HNO<sub>3</sub>). After total sample digestion, aliquots were taken for the subsequent  
155 determination of Zn concentrations and isotopic compositions.

156 Aliquots of sediments samples were leached using 0.1 M acetate to remove weakly-  
157 sorbed metal species (Quevauviller et al., 1997; Rauret et al., 1999, Gleyzes et al., 2002).  
158 To this end, about 500 mg of sediment were weighted in tube flacons and 17.5 ml of 0.1 M  
159 acetate were added. The sediment and acetate mixtures were shaken for 16 hours at 30±10  
160 rpm. The solutions were centrifuged at 3000 g for 20 min and the supernatants were filtered  
161 using a syringe and membrane filter (0.22 µm). The filtered solutions were stored at 4 °C  
162 until analysis day.

163 All acids used during the cleaning of bottles and lab ware and during the sample  
164 preparation were distilled by sub-boiling in Teflon™ stills. The water used was < 18.2

165 M $\Omega$  (Nanop System®). The chemical procedures were performed at the clean laboratory  
166 suites at the University of São Paulo (USP) and the University of Brasília (UnB).

167

### 168 **3.2 Elemental and isotope ratio analysis of zinc**

169 Aluminum, Fe, Ti, Ca, Mg, P, Mn, Zn, Cu, Ni and Cr were analyzed using inductively  
170 coupled plasma optic emission spectrometry (ICP-OES, Spectro Ciros Vision, Spectro, at  
171 Campo Laboratory, Minas Gerais, Brazil). Multi-elemental standard solutions (Merck®)  
172 were used to produce external calibration curves. Certified reference materials (BHVO-2  
173 and BCR-2 basalts from the USGS; 1646a estuarine sediment and 1573a tomato leaves  
174 from the NIST) were used to assess the accuracy of analysis. The accuracy expressed as  
175 percentage relative error was always within 10% of the certified values for all the elements  
176 studied.

177 Before the isotope ratio determinations, Zn was separated from other elements using  
178 an ion-exchange chromatography procedure employing a Bio-Rad PolyPrep column filled  
179 with 2 ml of the anion exchange resin AG-MP1, 100-200 mesh, (Araújo et al., 2017b). For  
180 subsequent mass bias corrections, the Cu standard NIST-976 was added to the purified  
181 fractions after the ion exchange procedure and concentration matched with the ratio 1:1  
182 (300  $\mu\text{g ml}^{-1}$  in 0.05 M  $\text{HNO}_3$ ). Zinc isotopic ratios were measured using a  
183 ThermoFinnigan Neptune MC-ICP-MS at the Laboratório de Geocronologia of the  
184 University of Brasília and at the Laboratorio de Geocronologia of the University of Sao  
185 Paulo. The introduction interface consisted of quartz glass spray chamber (cyclone +  
186 standard Scott double pass) coupled with a low flow PFA nebulizer (50  $\mu\text{l min}^{-1}$ ). The  
187 analytical sequences ran automatically using a Cetac ASX-100 autosampler and low mass  
188 resolution collector slits.

189 The zinc isotopes ratios were measured relative to the in-house single element  
 190 standard MERCK Lot #9953 labeled henceforward as Zn<sub>UnB</sub> standard. The standard-sample  
 191 bracketing technique was used, i.e., each sample was bracketed by standard solution  
 192 mixture (Zn<sub>UnB</sub> and Cu<sub>NIST-976</sub>) with rinses between sample and standard analyses with 3 %  
 193 (v/v) HNO<sub>3</sub>. The raw ratios were corrected for instrumental mass fractionation using the  
 194 exponential law based and the certified ratio (<sup>65</sup>Cu/<sup>63</sup>Cu = 0.4456) for Cu of the NIST SRM  
 195 976 standard.

196 The δ<sup>66</sup>Zn values were calculated as the deviation of the mass bias corrected isotope  
 197 ratio of the samples from the mean of the mass bias-corrected isotopes ratios of the  
 198 bracketing standards:

$$200 \quad \delta^{66}\text{Zn}(\text{‰}) = \left( \frac{{}^{66}\text{Zn}/{}^{64}\text{Zn}_{\text{sample}}}{{}^{66}\text{Zn}/{}^{64}\text{Zn}_{\text{standard}}} - 1 \right) \text{ eq.1}$$

201  
 202 Zinc isotope data reported in this study are expressed relative to the Johnson Matthey  
 203 Company 3-0749-L (JMC<sub>3-0749-L</sub>) reference standard calibrated against our Zn<sub>UnB</sub> standard  
 204 (ΔZn<sub>JMC-UnB</sub> = +0.17 ‰). For analytical quality control, the certified isotope reference  
 205 material Zn IRMM-3702 was measured two or three times along each session analysis  
 206 yielding a δ<sup>66</sup>Zn<sub>JMC</sub> value of -0.27 ± 0.06 ‰ (n=30, 2σ). This value agrees with values the  
 207 average value of compiled data from other laboratories (+0.30 ± 0.01, 2SE, Moynier et al.,  
 208 2017). The 1573a tomato leaves showed δ<sup>66</sup>Zn<sub>JMC</sub> values of +0.79 ± 0.09 ‰ (2σ, n=4). The  
 209 δ<sup>66</sup>Zn<sub>JMC</sub> values obtained for BHVO-2 basalt (+0.25 ± 0.10‰, 2σ, n=5), BCR-2 basalt  
 210 (+0.25 ± 0.08‰, 2σ, n=1), and AGV-2 andesite (+0.29 ± 0.07, 2σ, n=2) are in line with  
 211 those reported in the literature for silicate rocks (Chen et al., 2013; Sossi et al., 2015).

212 Average reproducibility for  $\delta^{66}\text{Zn}_{\text{JMC}}$  values determined for the certified reference material  
213 Zn IRMM-3702 and unknown samples was  $\pm 0.06\text{‰}$  ( $2\sigma$ ). This value was taken to represent  
214 the external reproducibility of the method.

215

#### 216 4. Results

217 The analytical results for the mangrove superficial sediments and leaves are shown in Table  
218 1. Highest Zn concentrations (expressed in  $\mu\text{g g}^{-1}$ ,  $1\sigma$ ,  $n=3$ ) in surface sediments are found  
219 at station A ( $21,551 \pm 2072$ ), while intermediate values are found in station C ( $316 \pm 112$ ),  
220 and the lowest values in station B ( $164 \pm 17$ ). The sediment samples of Sepetiba Bay display  
221 a wide range of  $\delta^{66}\text{Zn}_{\text{JMC}}$  values (between  $+0.36$  and  $+0.84\text{‰}$ , Table 1). Samples from Saco  
222 do Engenho mangroves (station A) exhibit the highest values, ranging between  $+0.80$  and  
223  $+0.84\text{‰}$  (Fig. 2) with an average of  $+0.82 \pm 0.04\text{‰}$  ( $n=3$ ). Surface sediments collected in  
224 the mangrove close to the São Francisco Channel (station B) display  $\delta^{66}\text{Zn}_{\text{JMC}}$  values  
225 between  $+0.44$  and  $+0.49\text{‰}$  (average of  $+0.47 \pm 0.04\text{‰}$  ( $n=3$ ), slightly heavier than values  
226 found in the mangrove of Enseada das Garças (station C) which range between  $+0.36$  to  
227  $+0.42 \pm \text{‰}$  (Fig.2) with an average of  $+0.39 \pm 0.06\text{‰}$  ( $n=3$ ). Zinc concentrations ( $\mu\text{g g}^{-1}$ ,  $1\sigma$ ,  
228  $n=3$ ) in the exchangeable fraction (0.1 M acetate leach) were  $8836 \pm 1788$ ,  $71 \pm 19$  and  $173$   
229  $\pm 94$  ( $n=3$ ) for the mangrove stations A, B, C, respectively. This corresponds to 41, 43 and  
230 55% of the bulk sediment Zn concentration.

231 Average Zn concentrations in *L. racemosa* leaves in the mangrove stations follow  
232 the same trend observed for sediments, i.e. the highest concentrations ( $\mu\text{g g}^{-1}$ ,  $1\sigma$ ,  $n=3$ ) are  
233 found in station A ( $47 \pm 5$ ), followed by station C ( $25 \pm 2$ ) and station B ( $15 \pm 2$ ) (Fig.2). The  
234 leaves collected at the stations with higher Zn concentrations in sediments (stations A and  
235 C) display similar  $\delta^{66}\text{Zn}$  values of  $+0.09 \pm 0.04\text{‰}$  and  $+0.08 \pm 0.10\text{‰}$  ( $\pm 2\sigma$ ,  $n=3$ ),

236 respectively (Fig.2). These values are very different from those observed in leaves from  
237 station B, which display heavier  $\delta^{66}\text{Zn}$  values of  $+0.23 \pm 0.02\%$  ( $2\sigma$ ,  $n=3$ , Fig.2).

238

## 239 **5. Discussion**

### 240 **5.1 Zinc isotope composition of end-members from Sepetiba Bay**

241 Two previous studies of our group (Araújo et al., 2017a,c) assessed the variability of the Zn  
242 isotope values within a single sediment core and of suspended particulate matter collected  
243 in the estuary. We found that the isotope signatures in the sediment core can be accounted  
244 for by mixing of three main end-members: a terrestrial detrital source ( $\delta^{66}\text{Zn}_{\text{JMC}} = +0.28$   
245  $\pm 0.12\%$ ,  $2\sigma$ ), a marine detrital source ( $\delta^{66}\text{Zn}_{\text{JMC}} = +0.45 \pm 0.03\%$ ,  $2\sigma$ ), and an  
246 anthropogenic source associated with electroplating wastes released into the bay ( $\delta^{66}\text{Zn}_{\text{JMC}}$   
247  $= +0.86 \pm 0.15\%$ ,  $2\sigma$ , Araújo et al., 2017a; Araújo et al., 2017c). Table 2 summarizes  
248 relevant data compiled from Araújo et al. (2017a), including the Zn isotopic signatures of  
249 top layers (~5 cm) from sediment cores of mud flat sediments collected close the stations  
250 A, B and C determined in this study. The compiled dataset is used in the following sections  
251 to support the interpretations of the new dataset in the mangrove systems presented in this  
252 study.

253

### 254 **5.2 Tracing anthropogenic zinc sources in the mangrove sediments**

255  $\delta^{66}\text{Zn}_{\text{JMC}}$  values of the surface sediments at Saco do Engenho (station A) range between  
256  $+0.72$  and  $+1.15\%$  (Araújo et al., 2017a). They are likely controlled by the isotope  
257 composition of waste derived from the electroplating plant as station A is located within the  
258 hot spot contamination area (Table 1). In addition, isotope values previously reported for  
259 waste and slag produced during metallurgical processes are in the same range ( $+0.59$  to

260 +1.49‰, Sivry et al., 2008; Juillot et al., 2011). The large isotope fractionation between  
261 electroplating waste and ores minerals (average of  $+0.03 \pm 0.24\%$  for willemite, Araújo et  
262 al., 2017a) and concentrates ores of sphalerites from worldwide (average of  $+0.03 \pm 0.1\%$ ,  
263 Ochoa et al., 2016) may be associate to the electrochemical separation process used during  
264 ore refining (Kavner et al., 2008; Yin et al., 2016).

265         Suspended particles enriched in Zn as well as dissolved Zn are transported from the  
266 hot spot area throughout the bay and deposited in the tidal flats and mangroves along the  
267 shore (Leal Neto et al. 2006; Roncarati and Carelli, 2012). There, dissolved metal  
268 contaminants including Zn and suspended particles are immobilized within organic-rich  
269 and anoxic sediment due to the formation of insoluble metallic sulfides and complexes with  
270 organic matter (Machado et al., 2008; Andrade et al., 2012; Ribeiro et al., 2013). This metal  
271 trapping capacity likely explains the moderate to high concentrations of Zn in stations B  
272 and C, even though the latter station is located as far as 16 km from the old electroplating  
273 plant. Additional input from other anthropogenic sources (e.g., urban effluents) also could  
274 play a role.

275         The surface mangrove sediment from stations B and C show  $\delta^{66}\text{Zn}_{\text{JMC}}$  values  
276 between the geological background of Sepetiba Bay, estimated at  $+0.28 \pm 0.12\%$  ( $2\sigma$ ),  
277 represented by granites rocks and sediment core sections from pre-industrial period (Table  
278 2) and electroplating wastes, estimated at  $+0.86 \pm 0.12\%$  ( $2\sigma$ ) represented by waste from  
279 the old electroplating plant (Araújo et al., 2017a, Fig.2, Table 2). The mangroves of  
280 Sepetiba bay are known to act as sinks of the suspended particulate matter brought during  
281 the high tides (Lacerda et al., 1988). In Figure 3, we observe an overlap of the isotope  
282 signature between the first 5 cm layers of sediment cores of mud flat and mangrove surface  
283 sediments. This suggests that the Zn isotope compositions of suspended particle material

284 and dissolved Zn remain unchanged during the transport and after deposition in the  
285 mangrove system. The lack of overlap in the station C may indicate inputs from an  
286 additional, unknown source in this mangrove system. This would well be in agreement with  
287 the location of and proximity of untreated urban sewage effluents observed during the field  
288 work.

289

### 290 **5.3 Zinc concentrations and isotope compositions of tree leaves**

291 The zinc isotope composition of the leaves of *L. racemosa* (ranging between +0.08 and  
292 +0.23‰) are lighter than that of the bulk sediments (ranging between +0.36 to +0.84‰).

293 The smaller variation of  $\delta^{66}\text{Zn}$  found in the leaves is possibly due to an isotopically more  
294 homogenous bioavailable pool (see discussions further below). The leaves collected at the  
295 stations with higher Zn concentrations in the surface sediments (stations A and C) display  
296 similar  $\delta^{66}\text{Zn}$  values ( $+0.09 \pm 0.04\text{‰}$  and  $+0.08 \pm 0.10\text{‰}$ ,  $\pm 2\sigma$ ,  $n=3$ ) but are significant  
297 different from those observed in leaves of trees collected at station B ( $+0.23 \pm 0.02\text{‰}$ ,  $2\sigma$ ,  
298  $n=3$ , Fig.2). As will be discussed later, this difference between mangrove sites can be  
299 associated to physiological responses and tolerance mechanisms of mangrove trees.

300

#### 301 **5.3.1 Suggested control of mineral phases and rhizosphere processes**

302 The changes in Zn concentrations in *L. racemosa* leaves reflect changes in Zn  
303 concentrations in surface sediments (Fig.2) though the magnitudes of increase or decrease  
304 is different. For example, we observe between the stations A and B a 100-fold increase in  
305 Zn concentrations in the sediments but only a 3-fold increase in the leaves. It is conceivable  
306 that the bioavailability of excess anthropogenic Zn is strongly reduced at station A. The

307 capability of mangroves to reduce metal bioavailability is attributed to the formation of  
308 stable metal sulfides, metal–organic matter complexes and sorption on clays minerals  
309 (Machado et al., 2005; Marchand et al., 2006; MacFarlane et al., 2007; Marchand et al.,  
310 2011; Lewis et al., 2011). The lower Zn concentrations in the leaves may also reflect  
311 tolerance mechanisms including root iron plaque formation, excretion through leaves or  
312 roots and compartmentation in root cells (Macfarlane and Burchett, 1999; MacFarlane and  
313 Buchett, 2000; MacFarlane and Burchett, 2002; Machado et al., 2005; MacFarlane et al.,  
314 2007; Naido et al., 2014). The large contribution of Zn in the exchangeable fraction, i.e.,  
315 from 41 to 55% (Table 1), suggests a weak role of the sediment on the retention of Zn and a  
316 prevailing of tolerance mechanisms on the reduction of Zn bioavailability.

317 Iron plaques formation is a critical process to control metal uptake via root. They  
318 are formed during oxidation of  $\text{Fe}^{2+}$  in anoxic, waterlogged conditions at the root surface by  
319  $\text{O}_2$  diffusing through the aerenchym (Machado et al., 2005; Aucour et al., 2017; Garnier et  
320 al., 2017). In Sepetiba Bay, a previous study of seedlings of *L. racemosa* showed that  
321 almost 90% of Zn in the roots are associated with iron plaque and only a minor fraction is  
322 stored in the root tissues (Machado et al, 2005). It is therefore likely that Zn adsorption on  
323 iron plaques is an important process with respect to isotope fractionation. Several  
324 laboratory studies have demonstrated significant Zn isotope fractionation during sorption  
325 processes on Fe-bearing phases with preferential enrichment of heavy isotope in the solid  
326 phase (Pokrovsky et al., 2005; Balistrieri et al., 2008; Juillot et al., 2008, Dekov 2010,  
327 2014). This would lead a preferential immobilization of heavy Zn isotopes on iron plaques,  
328 resulting in a Zn phyto-available pool isotopically lighter.

329 A second important reservoir of Zn in mangrove sediments are sulfide compounds  
330 formed during anoxic conditions by microbial activity. Previous studies demonstrated that

331 Zn sulfides are isotopically lighter compared to other mineral phases (John et al., 2008;  
332 Kelley et al., 2009; Veeramani et al., 2015; Jamieson-Hanes et al., 2017) and Aucour and  
333 co-workers (2016) found enrichment of light Zn isotopes in roots compared to the soil in a  
334 wetland system in France, due to the dissolution of ZnS enriched in light isotopes.

335 Mangroves are subjected to daily redox changes triggered by tidal cycles and  
336 bioturbation processes. This leads to re-precipitation and re-dissolution of mineral phases.  
337 In anoxic conditions (e.g., during high tides), Fe-oxyhydroxides are partially reduced and  
338 dissolved releasing metals into solution, while sulfides produced from the microbial  
339 activity immobilize metals. During oxic conditions, sulfides may be oxidized releasing  
340 metals to pore- or column water (Huerta-Diaz and Morse, 1992; Marchand et al., 2011;  
341 Andrade et al., 2012; Machado et al., 2014). Previous mineralogical analyses (XRD) of the  
342 mangrove sediments in Sepetiba bay showed presence of ankerite ( $\text{Ca}(\text{Fe},\text{Mg},\text{Mn})(\text{CO}_3)_2$ )  
343 and pyrite, evidencing an intense redox cycling of Fe and Mn during diagenetic processes  
344 involving carbon-iron-sulfur interactions and microbial metabolism (Araújo et al., 2017d).

345 The changes in sedimentary mineralogy induced by diagenetic processes, tidal  
346 cycles and bioturbation affects the Zn mobility in the sediment/water interface and its  
347 isotope compositions (Veeramani et al., 2015; Jamieson-Hanes et al., 2017, Deckov et al.,  
348 2010, 2014). A flow-through cell experiment designed for the study of Zn speciation *in situ*  
349 in natural sediments demonstrated an enrichment of the heavier Zn isotope in the aqueous  
350 phase due to the continuous Zn removal via microbially-mediated ZnS precipitation in  
351 reducing conditions (Jamieson-Hanes et al., 2017). Leaching experiments of metallurgical  
352 slags showed different directions and extent of Zn isotope fractionation depending on the  
353 formation or dissolution of secondary phases such as carbonates, hydroxides, or oxides  
354 during weathering (Yin et al., 2018). To predict accurately the overall magnitude or

355 direction of Zn isotope fractionation resulting from these various processes in mangrove  
356 sediments, however, remains difficult due to the wide variety of Zn bearing mineral phases.

357         Nevertheless, it is important to note that despite the wide range of Zn concentrations  
358 found in the sampled sediments, the Zn isotope compositions of the leaves displays a rather  
359 narrow range of  $\delta^{66}\text{Zn}_{\text{JMC}}$  values, varying between +0.08 and +0.23‰. This small range of  
360  $\delta^{66}\text{Zn}_{\text{JMC}}$  values suggests that the isotopic composition of the Zn pool available for uptake is  
361 similar at the different sites. This is supported by the isotope analysis of the exchangeable  
362 phase (data unpublished).

363

### 364 ***5.3.2 Zinc uptake and translocation to aerial parts of mangrove plants***

365 The enrichment of light isotopes in leaf tissues may be associated to the combined effects  
366 of biological isotope fractionation during Zn uptake and translocation to aerial parts of  
367 mangrove plants. The direction and magnitude of the Zn isotope fractionation during Zn  
368 uptake is depending of Zn speciation and uptake mechanisms (Jouvin et al., 2012). The  
369 enrichment of the light isotope in the leaves of *L. racemosa* found in this study is in line  
370 with uptake of free  $\text{Zn}^{2+}$  via diffusion. The transport of Zn from root to shoot and leaves in  
371 higher plants occurs via the xylem sap, which seems, in general, to lead an enrichment of  
372 light isotopes in the leaves of high plants (Caldelas and Weiss, 2016) possibly due to ion  
373 exchange processes (Moynier et al., 2009).

374         It is also evident that sampling sites with medium (station C) and high (station A)  
375 degrees of Zn contaminations show lighter isotope compositions than the mangrove station  
376 with the lowest contamination degree (station B) (Fig.2). To explain this observation, we  
377 suggest physiological responses and tolerance mechanisms of mangrove trees as controlling  
378 process. Mangroves plants exclude metals or regulate uptake of metals at the root level and

379 limit translocation to the shoot to maintain the concentration of metals within physiological  
380 limits. This involves the use metallothioneins, phytochelatins and Cys-rich membrane  
381 proteins for metal transport, chelation, compartmentalization, exclusion and sequestration  
382 processes (Zhou and Goldsbrough, 1995; Cobbett, 2000; Hasan et al., 2017; Weng et al.,  
383 2012). Thus, Zn isotope compositions of leaves will reflect the various mechanisms that  
384 control uptake, accumulation, trafficking and detoxification of metals (MacFarlane et al.,  
385 2007; Da Souza et al., 2014; Arrivabene et al., 2016). Zinc complexation with organic  
386 ligands containing O and N donor atoms favor the heavy isotopes and the magnitude of Zn  
387 isotope fractionation during complexation seems proportional to the affinity constant  
388 (Markovic et al., 2017). Hence, complexation to organic ligands with O and N donor atoms  
389 could lead to the immobilization of heavy isotopes in cell roots and stems with a  
390 subsequent preferential translocation of light isotopes to aerial parts of plants. Sulphur  
391 containing molecules (cys-rich proteins, phyto-chelatins, metallo-thioneins) are likely also  
392 involved in membrane transport, chelation, compartmentalization, exclusion and  
393 sequestration processes of metals (Zhou and Goldsbrough, 1995; Cobbett, 2000; Weng et  
394 al., 2012, Fuji et al., 2014, Hasan et al., 2017), further imparting significant isotope  
395 fractionation.

396 Different Zn isotope signature patterns in plants as response to high or low Zn  
397 supplies have been reported in the literature. Caldelas et al. (2011) pioneered experiments  
398 with wetland plants (*Phragmites australis*) in substrates with toxic levels of Zn and  
399 observed heavier isotopic compositions in roots than in leaves. Similar observations were  
400 made studying plants grown in soils contaminated by metallurgic waste (Couder et al.,  
401 2016). Both groups suggested that under conditions of high Zn supplies, Zn is immobilized

402 by organic ligands and stored in cell organelles (e.g., vacuoles) leading to preferential  
403 accumulation of the heavy isotope of Zn excess in the roots.

404 Mangrove trees across genera and families tend to accumulate higher amounts in  
405 roots than leaves (MacFarlane et al., 2007) as detoxification mechanism. This would  
406 increase the enrichment of the light isotope in the Zn pool translocated to aerial plant  
407 compartments. Thus, metal stress should lead to different isotope patterns of mangrove  
408 leaves than those observed under normal conditions.

409

## 410 **6. Conclusions**

411 Mangrove ecosystems play an important role in the dynamics of metal contaminants in  
412 coastal areas. This work demonstrates that Zn isotopes is useful to trace anthropogenic  
413 sources in superficial mangrove sediments, especially, those associated to metallurgical  
414 pollution. We demonstrate that post-depositional biogeochemical processes do not  
415 significantly fractionate zinc isotopes in surface sediments.

416 Zinc isotopes in mangrove tree leaves show significant fractionation compared to  
417 the sediments, likely as result of Zn uptake and translocation to aerial parts. The subtle  
418 isotopic signatures among mangrove stations may be associated to tolerance mechanisms  
419 employed by mangroves under high Zn exposure to exclude metals or regulate uptake of  
420 metals to maintain Zn levels within physiological limits. Therefore, Zn isotope  
421 compositions of leaves are not indicative of sources. However, changes in Zn isotope  
422 compositions of leaves may be potential indicators for responses of mangrove plants to  
423 environmental changes and changes in physiological status.

424

## 425 **Acknowledgements**

426 This work was financially supported by CNPQ (D.F. Araújo PhD grant, process:  
427 161944/2012-4 and 211238/2014-7) e MCTI 400029/2015-4 (post-doctoral grant) and by  
428 different scientific projects listed: Marie Curie International Research Staff Exchange  
429 Scheme Fellowship within the 7<sup>th</sup> European Community Framework Program (NIDYFICS,  
430 n°318123) and CNPq universal 445423/2014-5, CNPq-PQ 310750/2014-8, FAP-DF  
431 193.000.932/2015. This work benefited from the Ciência Sem Fronteiras program (C.  
432 Quantin and Patrick Seyler) PV: 406288/2015-1 and PVE 400329/2014-0. We thank the  
433 anonymous reviewers for their valuable comments and suggestions to improve the quality  
434 of the paper.

435

#### 436 **References**

437

- 438 Agardy T. and Alder J.(2003) Coastal Systems (chapter 19) In: *Ecosystems and human well-*  
439 *being*(eds. Alcamo J. and Bennett E.). Island Press, Washington, DC.
- 440 Adriano D. and Adriano D. (2001) *Trace elements in terrestrial environments*. Springer, New York.
- 441 Alongi D.M. (2017) Micronutrients and mangroves: Experimental evidence for copper limitation.  
442 *Limnology and Oceanography*, in press.
- 443 Alongi D., Wattayakorn G., Boyle S., Tirendi F., Payn C. and Dixon P. (2004) Influence of roots  
444 and climate on mineral and trace element storage and flux in tropical mangrove soils.  
445 *Biogeochemistry* 69, 105-123.
- 446 Andrade R., Sanders C., Boaventura G. and Patchineelam S. (2012) Pyritization of trace metals in  
447 mangrove sediments. *Environ Earth Sci* 67, 1757-1762.
- 448 Araújo D.F., Boaventura G.R., Machado W., Viers J., Weiss D., Patchineelam S., Ruiz I.,  
449 Rodrigues A., Babinski M. and Dantas E. (2017a) Tracing of anthropogenic zinc sources in  
450 coastal environments using stable isotope composition. *Chemical Geology* 449, 226-235.
- 451 Araújo D., Boaventura G., Viers J., Mulholland D., Weiss D., Araújo D., Lima B., Ruiz I., Machado  
452 W., Babinski M. and Dantas E. (2017b) Ion exchange chromatography and mass bias  
453 correction for accurate and precise Zn isotope ratio measurements in environmental Reference  
454 Materials by MC-ICP-MS. *Journal of the Brazilian Chemical Society* 28, 225-237.
- 455 Araújo, D.F.; Machado, W.; Dominik, W.; Mulholland, D.S.; Boaventura, G.R.; Viers, J.; Garnier, J.;  
456 Dantas, E.L.; Babinski, M. (2017c). A critical examination of the possible application of zinc  
457 stable isotope ratios in bivalve mollusks and suspended particulate matter to trace zinc  
458 pollution in a tropical estuary. *Environmental Pollution*, v. 226, p. 41-47.
- 459 Araújo, D.F., Peres, L.G.M., Yopez, S., Mulholland, D.S., Machado, W., Tonhá, M., Garnier, J.,  
460 (2017d). Assessing man-induced environmental changes in the Sepetiba Bay (Southeastern  
461 Brazil) with geochemical and satellite data. *Comptes Rendus - Geosci.* 349, 290–298.
- 462 Arnold T., Kirk G., Wissuwa M., Frei M., Zhao F., Mason T. And Weiss D. (2010) Evidence for the  
463 mechanisms of zinc uptake by rice using isotope fractionation. *Plant. Cell. Environ.* 33, 370-  
464 381.

- 465 Arnold T., Markovic T., Kirk G., Schönbacher M., Rehkämper M., Zhao F. and Weiss D. (2015)  
466 Iron and zinc isotope fractionation during uptake and translocation in rice (*Oryza sativa*)  
467 grown in oxic and anoxic soils. *C. R. Geosci.* 347, 397-404.
- 468 Aucour A.-M., Bedell J.-P., Queyron M., Magnin V., Testemale D. and Sarret G. (2015) Dynamics  
469 of Zn in an urban wetland soil-plant system: Coupling isotopic and EXAFS approaches.  
470 *Geochim. Cosmochim. Acta* 160, 55-69.
- 471 Aucour A. M., Bedell J. P., Queyron M., Tholé R., Lamboux A. and Sarret G. (2017) Zn Speciation  
472 and Stable Isotope Fractionation in a Contaminated Urban Wetland Soil-Typha latifolia  
473 System. *Environ. Sci. Technol.* 51, 8350-8358.
- 474 Balistrieri L. S., Borrok D. M., Wanty R. B. and Ridley W. I. (2008) Fractionation of Cu and Zn  
475 isotopes during adsorption onto amorphous Fe(III) oxyhydroxide: Experimental mixing of  
476 acid rock drainage and ambient river water. *Geochim. Cosmochim. Acta* 72, 311-328.
- 477 Barone, R.H.T.(1973). Perfil analítico do zinco. Ministério das Minas e Energia. Departamento  
478 Nacional da Produção Mineral. Bolteim nº26. Rio de Janeiro, Brasil.
- 479 Bayen S. (2012) Occurrence, bioavailability and toxic effects of trace metals and organic  
480 contaminants in mangrove ecosystems: A review. *Environment International* 48, 84-101.
- 481 Borrok D., Gieré R., Ren M. and Landa E. (2010) Zinc Isotopic Composition of Particulate Matter  
482 Generated during the Combustion of Coal and Coal + Tire-Derived Fuels. *Environmental*  
483 *Science & Technology* 44, 9219-9224.
- 484 Castro P. and Huber M. (2010) *Marine biology*. McGraw-Hill, New York.
- 485 Caldelas, C., and Weiss, D. J. (2016). Zinc Homeostasis and isotopic fractionation in plants: a  
486 review. *Plant and Soil*, 1(411), 17-46.
- 487 Caldelas C., Dong S., Araus J. and Jakob Weiss D. (2011) Zinc isotopic fractionation in *Phragmites*  
488 *australis* in response to toxic levels of zinc. *J. Exp. Bot.* 62, 2169-2178.
- 489 Chen H., Savage P., Teng F., Helz R. and Moynier F. (2013) Zinc isotope fractionation during  
490 magmatic differentiation and the isotopic composition of the bulk Earth. *Earth Planet. Sci.*  
491 *Letters.* 369-370, 34-42.
- 492 Clemens S. (2001) Molecular mechanisms of plant metal tolerance and homeostasis. *Planta* 212,  
493 475-486.
- 494 Cobbett C. S. (2000) Phytochelatins and their roles in heavy metal detoxification. *Plant Physiol.*  
495 123, 825-832.
- 496 Couder E., Mattielli N., Drouet T., Smolders E., Delvaux B., Iserentant A., Meeus C., Maerschalk  
497 C., Opfergelt S. and Houben D. (2015) Transpiration flow controls Zn transport in *Brassica*  
498 *napus* and *Lolium multiflorum* under toxic levels as evidenced from isotopic fractionation. *C.*  
499 *R. Geosci.* 347, 386-396.
- 500 Coutaud A., Meheut M., Viers J., Rols J. and Pokrovsky O. (2014) Zn isotope fractionation during  
501 interaction with phototrophic biofilm. *Chemical Geology* 390, 46-60.
- 502 Da Souza I., Bonomo M. M., Morozesk M., Rocha L. D., Duarte I. D., Furlan L. M., Arrivabene H.  
503 P., Monferrán M. V., Matsumoto S. T., Milanez C. R. D., Wunderlin D. A. and Fernandes M.  
504 N. (2014) Adaptive plasticity of *Laguncularia racemosa* in response to different environmental  
505 conditions: Integrating chemical and biological data by chemometrics. *Ecotoxicology* 23, 335-  
506 348.
- 507 Dekov, V.M., Cuadros, J., Kamenov, G.D., Weiss, D., Arnold, T., Basak, C., Rochette, P.,  
508 2010. Metalliferous sediments from the H.M.S. Challenger voyage (1872-1876).  
509 *Geochim. Cosmochim. Acta* 74, 5019-5038. doi:10.1016/j.gca.2010.06.001
- 510 Dekov, V.M., Vanlierde, E., Billström, K., Garbe-Schönberg, C.D., Weiss, D.J., Gatto  
511 Rotondo, G., Van Meel, K., Kuzmann, E., Fortin, D., Darchuk, L., Van Grieken, R.,  
512 2014. Ferrihydrite precipitation in groundwater-fed river systems (Nete and Demer  
513 river basins, Belgium): Insights from a combined Fe-Zn-Sr-Nd-Pb-isotope study.  
514 *Chem. Geol.* 386, 1-15. doi:10.1016/j.chemgeo.2014.07.023

- 515 Garnier J., Garnier J. M., Vieira C. L., Akerman A., Chmeleff J., Ruiz R. I. and Poitrasson F. (2017)  
516 Iron isotope fingerprints of redox and biogeochemical cycling in the soil-water-rice plant  
517 system of a paddy field. *Sci. Total Environ.* 574, 1622–1632.
- 518 Gleyzes C., Tellier S. and Astruc M. (2002) Fractionation studies of trace elements in contaminated  
519 soils and sediments: A review of sequential extraction procedures. *TrAC - Trends Anal. Chem.*  
520 **21**, 451–467.
- 521 Giri, C., Ochieng, E., Tieszen, L. L., Zhu, Z., Singh, A., Loveland, T. Masek, J. and Duke, N.  
522 (2011). Status and distribution of mangrove forests of the world using earth observation  
523 satellite data. *Global Ecology and Biogeography*, 20(1), 154-159.
- 524 Hasan M. K., Cheng Y., Kanwar M. K., Chu X.-Y., Ahammed G. J. and Qi Z.-Y. (2017) Responses  
525 of Plant Proteins to Heavy Metal Stress—A Review. *Front. Plant Sci.* 8.
- 526 Jamieson-Hanes J. H., Shrimpton H. K., Veeramani H., Ptacek C. J., Lanzirotti A., Newville M. and  
527 Blowes D. W. (2017) Evaluating zinc isotope fractionation under sulfate reducing conditions  
528 using a flow-through cell and in situ XAS analysis. *Geochim. Cosmochim. Acta* 203, 1–14.
- 529 John S. G., Rouxel O. J., Craddock P. R., Engwall A. M. and Boyle E. a. (2008) Zinc stable  
530 isotopes in seafloor hydrothermal vent fluids and chimneys. *Earth Planet. Sci. Lett.* 269, 17–  
531 28.
- 532 Jouvin D., Louvat P., Juillot F., Maréchal C. N. and Benedetti M. F. (2009) Zinc isotopic  
533 fractionation: Why organic matters. *Environ. Sci. Technol.* 43, 5747–5754.
- 534 Jouvin D., Weiss D. J., Mason T. F. M., Bravin M. N., Louvat P., Zhao F., Ferec F., Hinsinger P.  
535 and Benedetti M. F. (2012) Stable isotopes of Cu and Zn in higher plants: Evidence for Cu  
536 reduction at the root surface and two conceptual models for isotopic fractionation processes.  
537 *Environ. Sci. Technol.* 46, 2652–2660.
- 538 Juillot F., Maréchal C., Ponthieu M., Cacaly S., Morin G., Benedetti M., Hazemann J. L., Proux O.  
539 and Guyot F. (2008) Zn isotopic fractionation caused by sorption on goethite and 2-Lines  
540 ferrihydrite. *Geochim. Cosmochim. Acta* 72, 4886–4900.
- 541 Kavner A., John S., Sass S. and Boyle E. (2008) Redox-driven stable isotope fractionation in  
542 transition metals: Application to Zn electroplating. *Geochimica et Cosmochimica Acta* 72,  
543 1731-1741.
- 544 Kelley K. D., Wilkinson J. J., Chapman J. B., Crowther H. L. and Weiss D. J. (2009) Zinc isotopes  
545 in sphalerite from base metal deposits in the Red Dog district, northern Alaska. *Econ. Geol.*  
546 104, 767–773.
- 547 Lacerda L. D. De, Pfeiffer W. C. and Fiszman M. (1987) Heavy metal distribution, availability and  
548 fate in Sepetiba Bay, S.E. Brazil. *Sci. Total Environ.* 65, 163–173.
- 549 Lacerda, L. D., Martinelli, L. A., Rezende, C. E., Mozeto, A. A., Ovalle, A. R. C., Victoria, R. L., ...  
550 & Nogueira, F. B. (1988). The fate of trace metals in suspended matter in a mangrove creek  
551 during a tidal cycle. *Science of the Total Environment*, 75(2-3), 169-180.
- 552 Leal Neto A., Legey L., González-Araya M. and Jablonski S. (2006) A System Dynamics Model  
553 for the Environmental Management of the Sepetiba Bay Watershed, Brazil. *Environmental*  
554 *Management* 38, 879-888
- 555 Lewis M., Pryor R. and Wilking L. (2011) Fate and effects of anthropogenic chemicals in mangrove  
556 ecosystems: A review. *Environmental Pollution* 159, 2328-2346.
- 557 MacFarlane G. and Burchett M. (1999) Zinc distribution and excretion in the leaves of the grey  
558 mangrove, *Avicennia marina* (Forsk.) Vierh. *Environ. Exp. Bot.* 41, 167-175.
- 559 MacFarlane G. and Burchett M. (2000) Cellular distribution of copper, lead and zinc in the grey  
560 mangrove, *Avicennia marina* (Forsk.) Vierh. *Aquat. Bot.* 68, 45-59.
- 561 MacFarlane G. and Burchett M. (2002) Toxicity, growth and accumulation relationships of copper,  
562 lead and zinc in the grey mangrove *Avicennia marina* (Forsk.) Vierh. *Mar. Environ. Res.* 54,  
563 65-84.
- 564 MacFarlane G. R., Koller C. E. and Blomberg S. P. (2007) Accumulation and partitioning of heavy  
565 metals in mangroves: A synthesis of field-based studies. *Chemosphere* 69, 1454–1464.

- 566 Machado W., Gueiros B. B., Lisboa-Filho S. D. and Lacerda L. D. (2005) Trace metals in  
567 mangrove seedlings: Role of iron plaque formation. *Wetl. Ecol. Manag.* 13, 199–206.
- 568 Machado W., Lacerda, L. D. (2004) Overview of the Biogeochemical Controls and Concerns with  
569 Trace Metal Accumulation in Mangrove Sediments. In: *Environmental geochemistry in*  
570 *tropical and subtropical environments* (ed. L. D. Lacerda). Springer, Berlin.
- 571 Machado, W., Gueiros, B.B., Lisboa Filho, S.D., Lacerda, L.D. (2005) Trace metals in mangrove  
572 seedlings: role of iron plaque formation. *Wetlands Ecol Managem* 13, 199-206.
- 573 Machado W., Santelli R., Carvalho M., Molisani M., Barreto R. and Lacerda L. (2008) Relation of  
574 Reactive Sulfides with Organic Carbon, Iron, and Manganese in Anaerobic Mangrove  
575 Sediments: Implications for Sediment Suitability to Trap Trace Metals. *J. Coastal Res.* 4, 25-  
576 32.
- 577 Marchand C., Allenbach M. and Lallier-Vergès E. (2011) Relationships between heavy metals  
578 distribution and organic matter cycling in mangrove sediments (Conception Bay, New  
579 Caledonia). *Geoderma* 160, 444-456.
- 580 Marchand, C., Fernandez, J., Moreton, B., 2016. Trace metal geochemistry in mangrove sediments  
581 and their transfer to mangrove plants (New Caledonia). *Sci. Total Environ.* 562, 216-227.
- 582 Marchand C., Lallier-Vergès E., Baltzer F., Albéric P., Cossa D. and Baillif P. (2006) Heavy metals  
583 distribution in mangrove sediments along the mobile coastline of French Guiana. *Mar. Chem.*  
584 98, 1-17.
- 585 Marković T., Manzoor S., Humphreys-Williams E., Kirk G. J. D., Vilar R. and Weiss D. J. (2017)  
586 Experimental Determination of Zinc Isotope Fractionation in Complexes with the  
587 Phytosiderophore 2'-Deoxymugeneic Acid (DMA) and Its Structural Analogues, and  
588 Implications for Plant Uptake Mechanisms. *Environ. Sci. Technol.* 51, 98–107.
- 589 Mason R. (2013) *Trace metals in aquatic systems*. Willey-Blackwell, Oxford.
- 590 Montezuma P.N. (2012) Análise de prováveis fatores causadores do processo de assoreamento na  
591 Baía de Sepetiba-RJ. In: *Bacia hidrográfica dos Rios Guandu, da Guarda e Guandu-Mirim*.  
592 INEA, Rio de Janeiro.
- 593 Moynier F., Pichat S., Pons M., Fike D., Balter V. and Albarède F. (2009) Isotopic fractionation and  
594 transport mechanisms of Zn in plants. *Chem. Geol.* 267, 125-130.
- 595 Nagelkerken, I. S. J. M., Blaber, S. J. M., Bouillon, S., Green, P., Haywood, M., Kirton, L. G.,  
596 Meinecke, J.O., Pawlik, J., Penrose, H.M., Sasekumar, A., S. and Somerfield, P. J. (2008).  
597 The habitat function of mangroves for terrestrial and marine fauna: a review. *Aquatic*  
598 *Botany*, 89(2), 155-185.
- 599 Naidoo G., Hiralal T. and Naidoo Y. (2014) Ecophysiological responses of the mangrove *Avicennia*  
600 *marina* to trace metal contamination. *Flora – Morph., Distr. Funct., Ecol. Plants* 209, 63-72.
- 601 Ochoa Gonzalez, R., Strekopytov, S., Amato, F., Querol, X., Reche, C., Weiss, D., 2016.  
602 New Insights from Zinc and Copper Isotopic Compositions into the Sources of  
603 Atmospheric Particulate Matter from Two Major European Cities. *Environ. Sci.*  
604 *Technol.* 50, 9816–9824.
- 605 Ochoa Gonzalez R. and Weiss D. (2015) Zinc Isotope Variability in Three Coal-Fired Power Plants:  
606 A Predictive Model for Determining Isotopic Fractionation during Combustion.  
607 *Environmental Science & Technology* 49, 12560-12567.
- 608 Peel, K., Weiss, D., Sigg, L., 2009. Zinc isotope composition of settling particles as a proxy  
609 for biogeochemical processes in lakes: Insights from the eutrophic Lake Greifen,  
610 Switzerland. *Limnol. Oceanogr.* 54, 1699–1708. doi:10.4319/lo.2009.54.5.1699.
- 611 Pokrovsky O. S., Viers J. and Freyrier R. (2005) Zinc stable isotope fractionation during its  
612 adsorption on oxides and hydroxides. *J. Colloid Interface Sci.* 291, 192–200.
- 613 Quevauviller P., Rauret G., López-Sánchez J. F., Rubio R., Ure A. and Muntau H. (1997)  
614 Certification of trace metal extractable contents in a sediment reference material (CRM 601)  
615 following a three-step sequential extraction procedure. *Sci. Total Environ.* 205, 223–234.

- 616 Rauret G., López-Sánchez J. F., Sahuquillo A., Rubio R., Davidson C., Ure A. and Quevauviller P.  
617 (1999) Improvement of the BCR three step sequential extraction procedure prior to the  
618 certification of new sediment and soil reference materials. *J. Environ. Monit.* **1**, 57–61.  
619 Available at: <http://xlink.rsc.org/?DOI=a807854h>.
- 620 Ribeiro A., Figueiredo A., Santos J., Dantas E., Cotrim M., Cesar Lopes Figueira R., V. Silva Filho  
621 E. and Cesar Wasserman J. (2013) Combined SEM/AVS and attenuation of concentration  
622 models for the assessment of bioavailability and mobility of metals in sediments of Sepetiba  
623 Bay (SE Brazil). *Marine Pollution Bulletin* **68**, 55-63.
- 624 Roncarati, H. and Carelli; S.G (2012). Considerações sobre estado da arte dos processos geológicos  
625 cenozóicos atuantes na baía de Sepeitba. In Baía de Sepetiba: Estado da Arte. Rio de Janeiro:  
626 Corbã.
- 627 Thapalia A., Borrok D., Van Metre P. and Wilson J. (2015) Zinc Isotopic Signatures in Eight Lake  
628 Sediment Cores from Across the United States. *Environmental Science & Technology* **49**,  
629 132-140.
- 630 Sandilyan, S., & Kathiresan, K. (2014). Decline of mangroves—a threat of heavy metal poisoning in  
631 Asia. *Ocean & coastal management*, **102**, 161-168
- 632 Sivry Y., Riotte J., Sonke J., Audry S., Schafer J., Viers J., Blanc G., Freydier R. And Dupre B.  
633 (2008) Zn isotopes as tracers of anthropogenic pollution from Zn-ore smelters The Riou Mort-  
634 Lot River system. *Chemical Geology* **255**, 295-304.
- 635 Sparks D. (2005) Toxic Metals in the Environment: The Role of Surfaces. *Elements* **1**, 193-197.
- 636 Sossi, P. A., Halverson, G. P., Nebel, O., & Eggins, S. M. (2015). Combined separation of Cu, Fe  
637 and Zn from rock matrices and improved analytical protocols for stable isotope  
638 determination. *Geostandards and Geoanalytical Research*, **39**(2), 129-149.
- 639 Souza I., Bonomo M. M., Morozesk M., Rocha L. D., Duarte I. D., Furlan L. M., Arrivabene H. P.,  
640 Monferrán M. V., Matsumoto S. T., Milanez C. R. D., Wunderlin D. A. and Fernandes M. N.  
641 (2014) Adaptive plasticity of *Laguncularia racemosa* in response to different environmental  
642 conditions: Integrating chemical and biological data by chemometrics. *Ecotoxicology* **23**, 335–  
643 348.
- 644 Suhr N., Schoenberg R., Chew D., Rosca C., Widdowson M. and Kamber B. S. (2018) Elemental  
645 and isotopic behaviour of Zn in Deccan basalt weathering profiles: Chemical weathering from  
646 bedrock to laterite and links to Zn deficiency in tropical soils. *Sci. Total Environ.* **619–620**,  
647 1451–1463.
- 648 Valiela, I., Bowen, J. L. and York, J. K. (2001). Mangrove Forests: One of the World's Threatened  
649 Major Tropical Environments: At least 35% of the area of mangrove forests has been lost in  
650 the past two decades, losses that exceed those for tropical rain forests and coral reefs, two  
651 other well-known threatened environments. *Bioscience*, **51**(10), 807-815.
- 652 Veeramani H., Eagling J., Jamieson-Hanes J. H., Kong L., Ptacek C. J. and Blowes D. W. (2015)  
653 Zinc Isotope Fractionation as an Indicator of Geochemical Attenuation Processes. *Environ.*  
654 *Sci. Technol. Lett.*, [acs.estlett.5b00273](https://doi.org/10.1039/c5em00273a).
- 655 Viers J., Oliva P., Nonell A., Gélabert A., Sonke J. E., Freydier R., Gainville R. and Dupré B.  
656 (2007) Evidence of Zn isotopic fractionation in a soil-plant system of a pristine tropical  
657 watershed (Nsimi, Cameroon). *Chem. Geol.* **239**, 124–137.
- 658 Viers J., Prokushkin A. S., Pokrovsky O. S., Kirilyanov A. V, Zouiten C., Chmeleff J., Meheut M.,  
659 Chabaux F., Oliva P. and Dupré B. (2015) Zn isotope fractionation in a pristine larch forest on  
660 permafrost-dominated soils in Central Siberia. *Geochem. Trans.* **16**, 3.
- 661 Yin N., Sivry Y., Benedetti M., Lens P. and van Hullebusch E. (2016) Application of Zn isotopes in  
662 environmental impact assessment of Zn–Pb metallurgical industries: A mini review. *Applied*  
663 *Geochemistry* **64**, 128-135.
- 664 Weiss D., Mason T., Zhao F., Kirk G., Coles B. and Horstwood M. (2004) Isotopic discrimination  
665 of zinc in higher plants. *New Phytologist* **165**, 703-710.
- 666 Weng B., Xie X., Weiss D. J., Liu J., Lu H. and Yan C. (2012) *Kandelia obovata* (S., L.) Yong

- 667 tolerance mechanisms to Cadmium: Subcellular distribution, chemical forms and thiol pools.  
668 *Mar. Pollut. Bull.* 64, 2453–2460.
- 669 Wiederhold J. (2015) Metal Stable Isotope Signatures as Tracers in Environmental Geochemistry.  
670 *Environmental Science & Technology* 49, 2606-2624
- 671 Zhou J. and Goldsbrough P. (1995) Structure, organization and expression of the metallothionein  
672 gene family in *Arabidopsis*. *Mol. Gen. Genet. MGG* 248, 318–328.
- 673

**Table 1.** Analytical data set for mangrove surface sediments and *L. racemosa* leaf samples

Samples	$\delta^{66}\text{Zn}_{\text{JMC}}$	Zn (EF)	Zn ( $\mu\text{g g}^{-1}$ )	Ca (%)	Ti (%)	Fe (%)	Si (%)	Al (%)	K (%)	Mn ( $\mu\text{g g}^{-1}$ )	P ( $\mu\text{g g}^{-1}$ )
<i>Mangrove station A (Saco do Engenho)</i>											
Sediment A1	+0.80	364	21,387	0.5	0.6	10.3	20.2	12.1	1.1	255.1	877
Sediment A2	+0.82	362	19,566	0.4	0.6	10.2	18.7	11.1	1.1	308.0	887
Sediment A3	+0.84	395	23,700	0.5	0.6	10.6	20.3	12.3	1.2	543.8	1111
Leaves A*	+0.09 $\pm$ 0.04		47 $\pm$ 5								
Zn-exchangeable <sup>‡</sup>			8836 $\pm$ 1788 (41%)								
<i>Mangrove station B (São Francisco Channel)</i>											
Sediment B1	+0.49	3.0	151	1.0	1.1	3.8	32.1	10.5	3.2	364.3	759
Sediment B2	+0.44	3.5	183	1.1	1.5	4.7	29.2	10.7	2.9	440.5	350
Sediment B3	+0.47	3.3	158	1.3	1.1	3.7	30.2	9.7	2.9	359.5	789
Leaves B*	+0.08 $\pm$ 0.10		15 $\pm$ 2								
Zn-exchangeable <sup>‡</sup>			71 $\pm$ 19 (43%)								
<i>Mangrove station C (Enseada das Garças)</i>											
Sediment C1	+0.42	8.0	251	0.5	0.6	3.1	30.5	6.4	0.4	349.8	1022
Sediment C2	+0.40	8.5	445	0.7	0.6	4.7	21.8	10.7	1.0	341.2	1351
Sediment C3	+0.36	5.0	252	0.9	0.6	4.5	19.7	10.3	0.9	204.7	962
Leaves C*	+0.02 $\pm$ 0.02		25 $\pm$ 2								
Zn-exchangeable <sup>‡</sup>			173 $\pm$ 94 (55%)								

\*Average concentration and standard deviation ( $\sigma$ ) obtained from three different replicates. Each replicate is composed by leaves sampled from different trees.

<sup>‡</sup>Average concentration and standard deviation ( $\sigma$ ) obtained from 0.1 M acetate leaching from the three sediments collected in each mangrove station. Values in brackets correspond the percentage value relative to total Zn concentration.

**Table 2.** Zinc isotope composition (expressed using  $\delta^{66}\text{Zn}_{\text{JMC}}$ ) of the end-members and the mud flat sediments from Sepetiba Bay Data compiled from Araújo et al.(2017a).

<i>End-members</i>	$\delta^{66}\text{Zn}_{\text{JMC}} (2\sigma)$
Electroplating wastes	+0.86 $\pm$ 0.15‰
Terrestrial detrital material	+0.28 $\pm$ 0.12‰
Marine detrital material	+0.45 $\pm$ 0.03‰
<i>Mud flat sediments (top layers of mud flat cores)</i>	
Station A	+0.83 $\pm$ 0.06‰
Station B	+0.67 $\pm$ 0.06‰
Station C	+0.46 $\pm$ 0.06‰

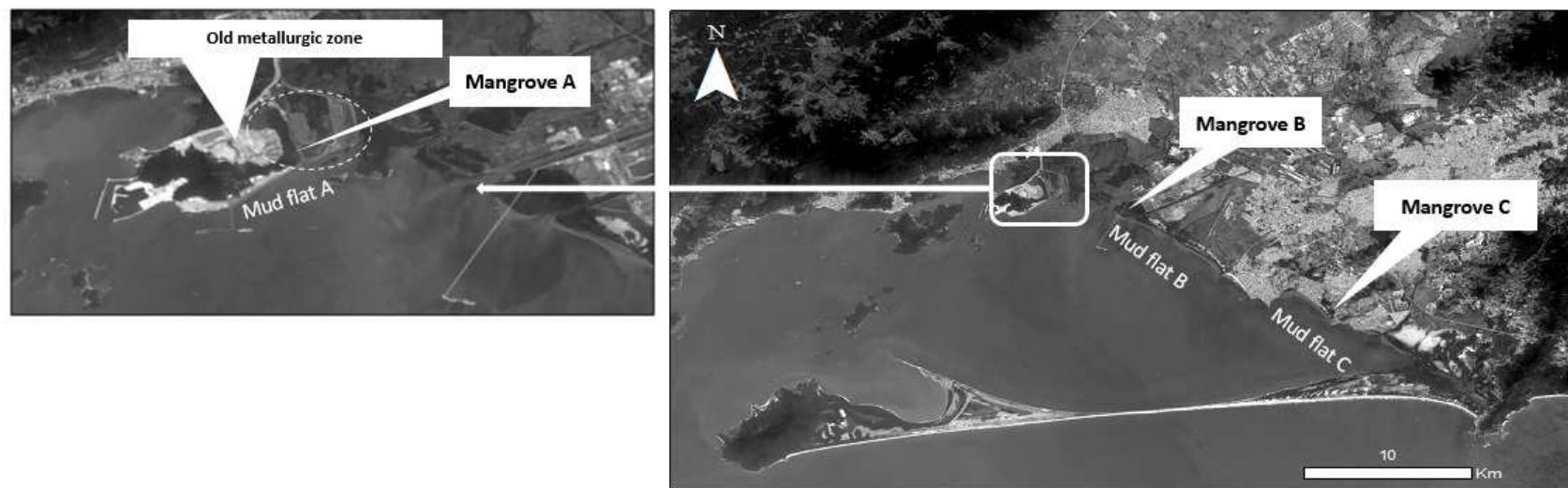


**Fig.1.** Map showing the sampling stations at the Sepetiba Bay. Station A: Saco do Engenho; station B: São Francisco Channel; station C: Enseada das Garças. Zinc isotope compositions of mud flat sediments are taken from Araújo et al. (2017) (Table 1). The insert at left shows the old metallurgic zone, where the electroplating activity operated from 1960's to end of 1990's. The dashed circle line highlight the Saco do Engenho mangrove, one site heavily impacted by the wastes lixiviated from the old wastes produced by the electroplating processes.

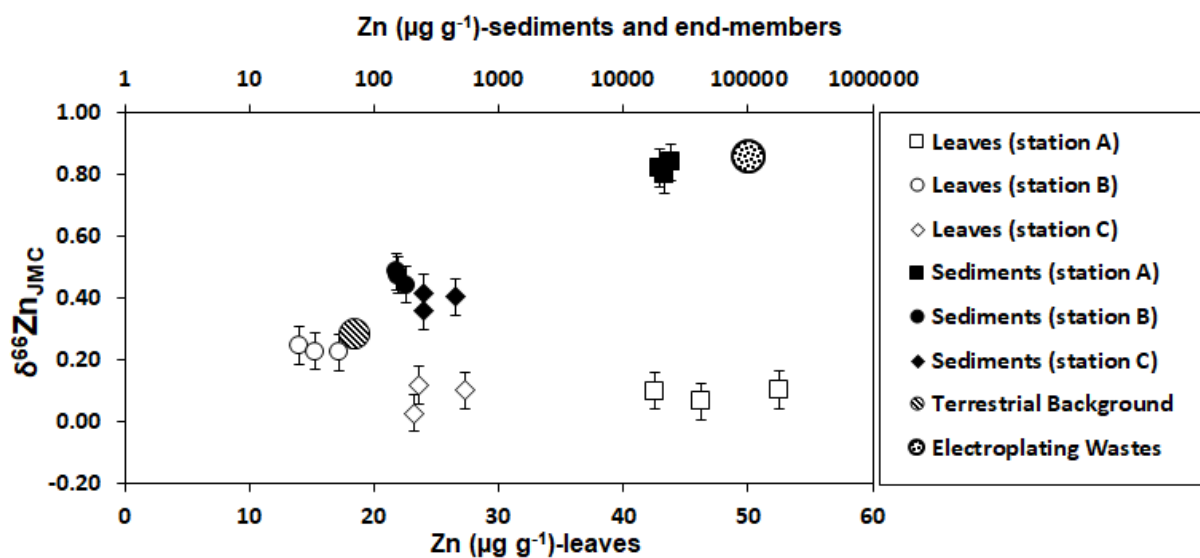


**Fig. 2.** Zinc isotope composition (expressed using  $\delta^{66}\text{Zn}_{\text{JMC}}$ ) and concentration of sediment and of leaves samples. The end-members (terrestrial detrital material and electroplating wastes) identified in a previous study performed by Araújo et al. (2017a) are included.

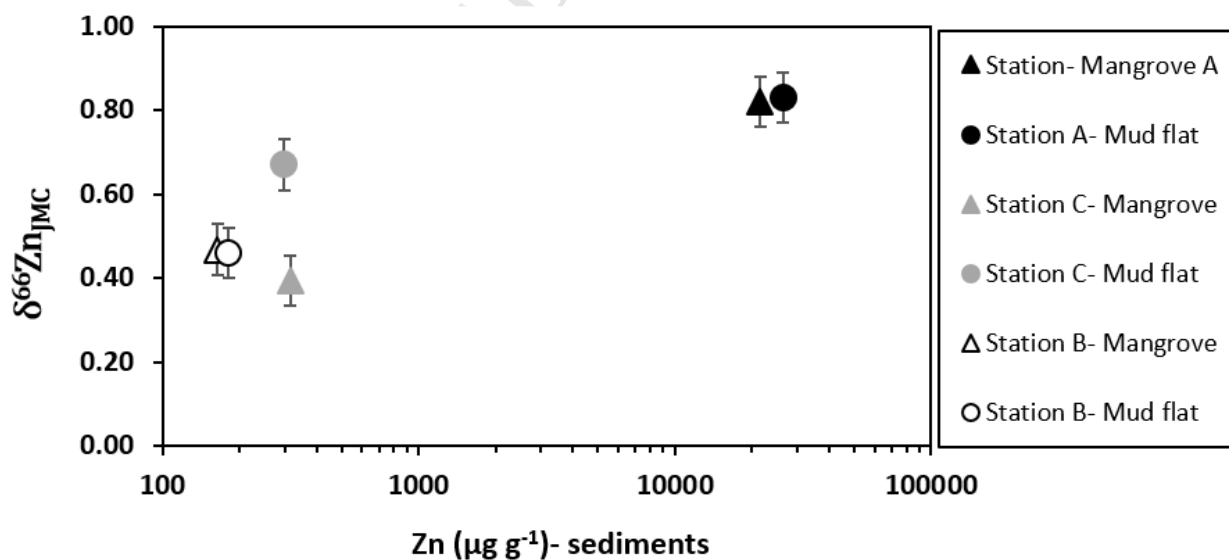


**Fig. 3.** Zinc isotope composition (expressed using  $\delta^{66}\text{Zn}_{\text{JMC}}$ ) of mangrove (this study) and mud flat (Araújo et al., 2017a) surface sediments (0-5 cm depth)